



## Approaching the full set of energy levels of water

Pavlo Maksyutenko, John S. Muentert, Nikolai F. Zobov, Sergei V. Shirin, Oleg L. Polyansky, Thomas R. Rizzo, and Oleg V. Boyarkin

Citation: *The Journal of Chemical Physics* **126**, 241101 (2007); doi: 10.1063/1.2748751

View online: <http://dx.doi.org/10.1063/1.2748751>

View Table of Contents: <http://scitation.aip.org/content/aip/journal/jcp/126/24?ver=pdfcov>

Published by the AIP Publishing

---

### Articles you may be interested in

Properties of the B<sup>+</sup>-H<sub>2</sub> and B<sup>+</sup>-D<sub>2</sub> complexes: A theoretical and spectroscopic study

J. Chem. Phys. **137**, 124312 (2012); 10.1063/1.4754131

The multistate multimode vibronic dynamics of benzene radical cation with a realistic model Hamiltonian using a parallelized algorithm of the quantumclassical approach

J. Chem. Phys. **130**, 144302 (2009); 10.1063/1.3108488

Computational investigation and experimental considerations for the classical implementation of a full adder on S O<sub>2</sub> by optical pump-probe schemes

J. Chem. Phys. **128**, 194308 (2008); 10.1063/1.2920486

A full analytic potential energy curve for the a  $\Sigma^+ 3$  state of KLi from a limited vibrational data set

J. Chem. Phys. **126**, 194313 (2007); 10.1063/1.2734973

Photodissociation of HOBr. I. Ab initio potential energy surfaces for the three lowest electronic states and calculation of rotational-vibrational energy levels and wave functions

J. Chem. Phys. **110**, 8448 (1999); 10.1063/1.478754

---



# NEW Special Topic Sections

**NOW ONLINE**  
Lithium Niobate Properties and Applications:  
Reviews of Emerging Trends

**AIP** Applied Physics Reviews

## Approaching the full set of energy levels of water

Pavlo Maksyutenko and John S. Muentert<sup>a)</sup>

*Laboratoire de Chimie Physique Moléculaire, École Polytechnique Fédérale de Lausanne, Station 6, CH-1015 Lausanne, Switzerland*

Nikolai F. Zobov, Sergei V. Shirin, and Oleg L. Polyansky

*Institute of Applied Physics, Russian Academy of Science, Uljanov Strasse 46, 603950 Niznii Novgorod, Russia*

Thomas R. Rizzo and Oleg V. Boyarkin<sup>b)</sup>

*Laboratoire de Chimie Physique Moléculaire, École Polytechnique Fédérale de Lausanne, Station 6, CH-1015 Lausanne, Switzerland*

(Received 2 May 2007; accepted 21 May 2007; published online 22 June 2007)

We report here the measurements of rovibrational levels in the electronic ground state of water molecule at the previously inaccessible energies above  $26\,000\text{ cm}^{-1}$ . The use of laser double-resonance overtone excitation extends this limit to  $34\,200\text{ cm}^{-1}$ , which corresponds to 83% of the water dissociation energy. We use experimental data to generate a semiempirical potential energy surface that now allows prediction of water levels with  $\text{sub-cm}^{-1}$  accuracy at any energy up to the new limit. © 2007 American Institute of Physics. [DOI: [10.1063/1.2748751](https://doi.org/10.1063/1.2748751)]

Water is undoubtedly one of the most important molecules in the universe, being involved in a variety of photochemical and photophysical processes on the Earth, the Sun,<sup>1</sup> and other cool stars.<sup>2</sup> As the major absorber of solar radiation, it plays a central role in the thermal balance of the Earth's atmosphere.<sup>3</sup> For an appropriate modeling of atmospheric radiative processes, the absorption spectrum of water vapor therefore must be known with high accuracy over the entire spectrum of solar radiation. Despite tremendous progress in molecular spectroscopy and atmospheric science, for the past 20 years this knowledge has been limited to the microwave, infrared, and visible spectral ranges, chiefly due to the experimental difficulty in accessing high-lying rovibrational levels. The residual near-UV range (280–400 nm), which still contains  $\sim 7.6\%$  of the incoming solar radiation,<sup>4</sup> remains the last “dark spot” within the spectrum of significant solar irradiance. It is also fundamental to understand the molecular motion of this benchmark triatomic, whose small size enables an accurate theoretical treatment. We report here experimental and theoretical results that break the 20 year old limit and expand our knowledge of rovibrational levels in water up to  $\sim 34\,200\text{ cm}^{-1}$ .

Thousands of transitions to levels with energies up to  $25\,500\text{ cm}^{-1}$  have been measured previously using Fourier transform spectroscopy<sup>5–7</sup> and laser techniques.<sup>8</sup> A great number of new absorption transitions, especially those originating from high rotational levels, have been detected by observing emission spectra from sunspots<sup>1</sup> as well as in laboratory experiments on hot water vapor.<sup>9</sup> Nevertheless, the upper limit of the identified rovibrational levels has not been improved significantly. While the recent use of highly sensi-

tive cavity ring down spectroscopy<sup>10</sup> has improved this limit to  $26\,270\text{ cm}^{-1}$ , the rovibrational levels above this energy have never been measured. Theory plays a central role in assigning measured spectra and it is capable to predict unmeasured transitions.<sup>11–14</sup> However, theoretical models need to be calibrated and, perhaps, adjusted by experiment for validation of their accuracy and limits of applicability. Having at least some experimentally determined energy levels through the energy region above  $26\,000$  is therefore crucial for an accurate prediction of numerous unmeasured levels.

As shown in Fig. 1, we use a double-resonance laser excitation to access high rovibrational states of  $\text{H}_2\text{O}$  in the electronic ground state.<sup>15,16</sup> A photon from the first laser (P1) promotes water vapor molecules in a particular rotational state to an intermediate level that contains four or five vibrational quanta in one of the OH stretches, via a vibrational overtone transition. The known rotational assignment of these transitions<sup>17</sup> allows us to determine the rovibrational identity of the intermediate levels. A photon of the second excitation laser (P2) subsequently promotes a fraction of these preexcited molecules to a higher rovibrational level containing between 8 and 12 OH-stretch quanta and between 0 and 1 quanta of OH bend.

Each overtone excitation step is governed by rotational selection rules, which strictly determine the change of angular momentum  $J(\Delta J=0, \pm 1)$  and its projection onto the  $z$  axis of the laboratory frame. Because rotational relaxation in our experiments is suppressed by using low pressure (50–100  $\mu\text{bars}$ ) and short delays (5–10 ns) between the excitation laser pulses, the known rotational identity of the originating level, along with rotational assignment of the intermediate state employed, leaves only a few options for rotational assignment of the terminal rovibrational states. In addition to rotational selection, the two-step excitation scheme allows an increase in the overall fraction of mol-

<sup>a)</sup>Permanent address: Department of Chemistry, University of Rochester, Rochester, NY 14627-0216

<sup>b)</sup>Author to whom correspondence should be addressed. Electronic mail: [oleg.boiarin@epfl.ch](mailto:oleg.boiarin@epfl.ch)

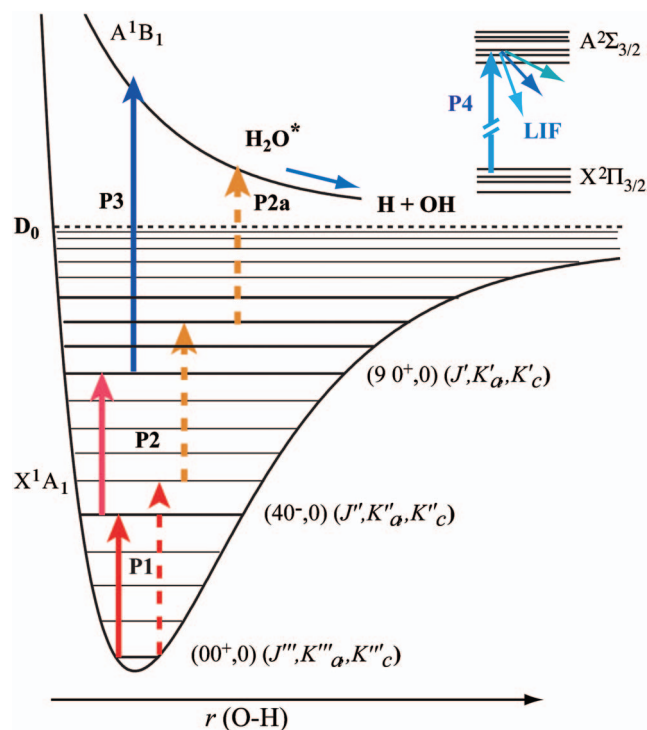


FIG. 1. (Color) Schematic energy level diagram of the double-resonance scheme for excitation of the OH stretch in  $\text{H}_2\text{O}$  (photons P1 and P2, shown by solid lines), with the subsequent electronic transition to the  $A^1B_1$  repulsive state by a photon P3 (solid line) of 355 nm for the  $(8,0)^+0$ ,  $(8,0)^+1$ , and  $(9,0)^+0$  bands or 532 nm for the  $(9,0)^+1$  and  $(10,0)^+0$  bands. Excitation of the  $(10,0)^+1$ ,  $(11,0)^+0$ ,  $(11,0)^+1$ , and  $(12,0)^+0$  bands (photons P1 and P2 shown by dashed lines) is followed by electronic excitation by a second photon (P2a, dashed line) of the second excitation laser. The subsequent prompt dissociation is followed by LIF detection of OH fragments. The vibrational label of the terminal state (in local mode notation) is indicative only.

ecules promoted to the terminal vibrational level by several orders of magnitude as compared to a single photon excitation from the ground vibrational state. Molecules in a terminal state are detected by vibrationally mediated photodissociation.<sup>18,19</sup> They first absorb an additional UV/visible photon (P3 or P2a) that brings them to the repulsive  $A^1B_1$  electronic state. Subsequent prompt dissociation yields OH fragments, which are detected via laser-induced fluorescence (LIF) using a fourth laser pulse (P4). Monitoring OH fluorescence as a function of wave number of the second laser pulse (P2), while keeping wave numbers of all other pulses fixed, generates a photofragment spectrum of an overtone transition from the intermediate level to a terminal one, as illustrated in Fig. 2. The total energy of a terminal level is the sum of the rovibrational energy of intermediate state, known with high accuracy,<sup>17</sup> and the energy of the subsequent excitation photon (P2), which we measure to  $<0.03 \text{ cm}^{-1}$  absolute accuracy. The measured 185 levels allow direct determination of the origins of 23 new vibrational bands shown in Table I.

Calculation of rovibrational energy levels in  $\text{H}_2\text{O}$  with ultimate accuracy would require the exact solution of the Schrödinger equation for the multiparticle system (three nuclei and ten electrons), which is currently impossible. One therefore uses the Born-Oppenheimer approximation, which

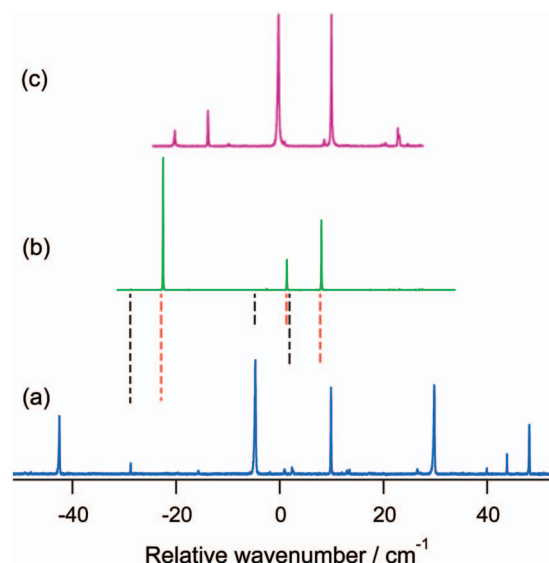


FIG. 2. (Color) Double-resonance excitation spectra of the (a) eighth, (b) ninth, and (c) eleventh vibrational overtone bands of the OH stretch in  $\text{H}_2\text{O}$ , plotted as a function of the total rovibrational energy and offset by 27 536, 29 866, and 33 853  $\text{cm}^{-1}$ , respectively. The spectra originate from single intermediate rovibrational states, prepared by the following transitions (a)  $[(4,0)^-0, (0,0,0)] \leftarrow [(0,0)0, (1,0,1)]$ , (b)  $[(4,0)^-0, (1,1,1)] \leftarrow [(0,0)0, (1,1,0)]$ , and (c)  $[(5,0)^-0, (0,0,0)] \leftarrow [(0,0)0, (1,0,1)]$ . The states are labeled by vibrational quantum numbers in local mode notation and by rotational quantum numbers  $J$ ,  $K_a$ , and  $K_c$ . Dashed lines below the spectrum (b) show two predictions of this spectrum, calculated employing the semiempirical surfaces  $\text{PES}_8$  (black) and  $\text{PES}_9$  (red).

separates electronic and nuclear motions, drastically reducing the complexity of the problem. Solving the electronic part of the Schrödinger equation is possible also only in some approximations, and we use one of the most accurate of them—multireference configuration interaction.<sup>13</sup> *Ab initio* electronic energies calculated at fixed nuclear geometries are fitted by an analytical function, which is then used as an *ab initio* potential energy surface (PES) to solve the Schrödinger equation for the nuclear degrees of freedom. One can solve this equation by a variational method to any accuracy,

TABLE I. Vibrational band origins in the electronic ground state of  $\text{H}_2\text{O}$ .

Band <sup>a</sup>	Energy ( $\text{cm}^{-1}$ )	Band <sup>a</sup>	Energy ( $\text{cm}^{-1}$ )
(5,3) <sup>-0</sup>	27 425.5(3) <sup>b</sup>	(10,0) <sup>-0</sup>	29 810.7(2) <sup>c</sup>
(6,1) <sup>-3</sup>	27 497.2(1) <sup>c</sup>	(9,1) <sup>+0</sup>	31 071.57 <sup>b</sup>
(6,1) <sup>+3</sup>	27 502.66 <sup>b</sup>	(9,1) <sup>-0</sup>	31 072.8(2) <sup>c</sup>
(9,0) <sup>-0</sup>	27 536.4(1) <sup>c</sup>	(10,0) <sup>+1</sup>	31 207.09 <sup>b</sup>
(9,0) <sup>+0</sup>	27 540.69 <sup>b</sup>	(10,0) <sup>-1</sup>	31 207.4(2) <sup>c</sup>
(7,1) <sup>-1</sup>	27 569.8(1) <sup>c</sup>	(11,0) <sup>+0</sup>	31 909.68 <sup>b</sup>
(7,1) <sup>+1</sup>	27 574.91 <sup>b</sup>	(11,0) <sup>-0</sup>	31 909.7(3) <sup>c</sup>
(7,1) <sup>+2</sup>	28 890.2(2) <sup>c</sup>	(11,0) <sup>+1</sup>	33 144.71 <sup>b</sup>
(7,1) <sup>-2</sup>	28 890.8(2) <sup>c</sup>	(11,0) <sup>-1</sup>	33 144.7(1) <sup>c</sup>
(9,0) <sup>+1</sup>	28 934.14 <sup>b</sup>	(12,0) <sup>+0</sup>	33 835.25 <sup>b</sup>
(9,0) <sup>-1</sup>	28 934.5(2) <sup>c</sup>	(12,0) <sup>-0</sup>	33 835.22 <sup>b</sup>
(10,0) <sup>+0</sup>	29 810.85 <sup>b</sup>		

<sup>a</sup>Local mode notation.

<sup>b</sup>Measured with absolute accuracy better than  $\pm 0.03 \text{ cm}^{-1}$ .

<sup>c</sup>Calculated with  $\text{PES}_{12}$  and corrected by the average deviation between energy of the measured and the calculated low  $J$  levels of the same band (with the uncertainty in parentheses), whenever  $J=0$  level has not been measured.



TABLE II. Comparison of measured and calculated energy levels.

Level	<i>Ab initio</i>			
	PES <sup>a</sup>	PES <sub>8</sub> <sup>b</sup>	PES <sub>9</sub> <sup>b</sup>	PES <sub>12</sub> <sup>b</sup>
$<26 \times 10^3 \text{ cm}^{-1c}$	1	0.03	0.04	0.08
$(9,0)^+0^d$	4.8	0.76	-0.27	-0.32
$(10,0)^+0^d$	10.5	6.36	0.65	-0.13
$(12,0)^+0^d$	48.3	49.5	8.5	0.03
$(26-34) \times 10^3 \text{ cm}^{-1c}$	...	...	...	0.24

<sup>a</sup>*Ab initio* PES of Ref. 13.<sup>b</sup>Semiempirical PES generated in this work by fitting to the measured levels lying, correspondingly, below 26 000, 27 800, and 34 000  $\text{cm}^{-1}$ .<sup>c</sup>Standard deviation (in  $\text{cm}^{-1}$ ) of all levels below  $26 \times 10^3 \text{ cm}^{-1}$  included in the fits.<sup>d</sup>Deviation (in  $\text{cm}^{-1}$ ) of the  $J=0$  level from the calculated value.<sup>e</sup>Standard deviation (in  $\text{cm}^{-1}$ ) for all measured levels included in the fits within  $(26-34) \times 10^3 \text{ cm}^{-1}$ .

limited by the basis set employed,<sup>20</sup> to obtain rovibrational energy levels and their wave functions. The accuracy of the surface determines how well such calculations reproduce spectroscopically determined energy levels.

Accounting for a variety of physical effects such as breakdown of the Born-Oppenheimer approximation, special relativity and quantum electrodynamics greatly improve the accuracy of the *ab initio* PES of water.<sup>13</sup> The solution of the Schrodinger equation for nuclear motions with that PES yields an average standard deviation of 1  $\text{cm}^{-1}$  in reproducing 17795 previously measured energy levels of  $\text{H}_2\text{O}$  isotopologues.<sup>21</sup> Comparing energy level calculations using this same *ab initio* surface to predict the newly measured levels in this work reveals a standard deviation of almost 50  $\text{cm}^{-1}$  in the region of 34 000  $\text{cm}^{-1}$  (Table II), reflecting the fact that this PES has not been designed for such high energy. It is clear that it must be improved significantly before being employed for assignment/prediction of transitions to energy levels in this region. Driven now by the availability of our new experimental data, one obvious step in this regard is to perform extensive calculations of *ab initio* points, including those for molecular geometries with large internuclear distances.

A complementary way to improve the accuracy of spectral calculations involves morphing the *ab initio* PES by multiplying it by an appropriate analytical function containing a set of parameters.<sup>22</sup> The resulting semiempirical PES is optimized by adjusting these parameters to minimize the deviation in fitting experimental energy levels. Applying this approach to the *ab initio* PES of Ref. 13 resulted in an average standard deviation of 0.08  $\text{cm}^{-1}$  in fitting the levels lying below 26 000  $\text{cm}^{-1}$ .<sup>14</sup> In the present work we first generate a new *ab initio* PES by fitting the 1149 recently calculated *ab initio* points<sup>21</sup> in addition to the previously known 346 points.<sup>13</sup> Morphing of this *ab initio* PES reduces the average standard deviation from 0.08 to 0.03  $\text{cm}^{-1}$  for levels below 26 000  $\text{cm}^{-1}$ . We then employ this new semiempirical surface (PES<sub>8</sub>) as a starting point, adding the newly measured levels to the fitting procedure band by band to generate another new PES that is capable to reproduce accurately all currently measured levels between the ground level and 34 200  $\text{cm}^{-1}$ . As a general rule, we include in the fit only

levels with  $J=0,2,5$  for each vibrational band.

Table II compares the discrepancy between the measured  $J=0$  level of the  $(9,0)^+,0$  vibrational band and that calculated using three different semiempirical surfaces. The use of the PES<sub>8</sub> drastically improves predictability for the  $v_{\text{str}}=9$  band in comparison with the *ab initio* PES, making possible a straightforward assignment of its complicated spectra [Fig. 2(a)]. Prediction of levels in the  $v_{\text{str}}=10$  band employing the PES<sub>8</sub> increases the deviation from the experiment by an order of magnitude, while including levels of the  $v_{\text{str}}=9$  band in the fit generates another surface (PES<sub>9</sub>) that brings the deviation back to the sub- $\text{cm}^{-1}$  scale [Fig. 2(b)]. The addition of 64 of our newly measured levels to the morphing procedure yields our final semiempirical surface (PES<sub>12</sub>), which results in an average standard deviation of 0.24  $\text{cm}^{-1}$  for these levels, improving it by orders of magnitude relative to the purely *ab initio* surface, although it is still eight times larger than the deviation obtained with the PES<sub>8</sub> for the fitted levels below 26 000  $\text{cm}^{-1}$ . This remaining inaccuracy suggests that the *ab initio* PES that we use to produce the semiempirical surfaces at high energy deviates sufficiently from the real PES that it becomes difficult to correct it through a morphing procedure. The development of a new, more accurate *ab initio* PES should therefore further improve semiempirical surfaces, reducing deviation of the fit values from experimental levels at high energies.

We also verified the ability of PES<sub>12</sub> to predict those of our measured levels that we did not include in the fit, in particular, those with high  $J$  rotational quantum number. Almost all these levels were predicted within  $\pm 0.5 \text{ cm}^{-1}$  accuracy, which is up to 100 times better than that of the *ab initio* predictions. We are thus confident that frequencies of most of the significant absorption transitions to the levels below  $\sim 34\,500 \text{ cm}^{-1}$  can now be predicted with similar accuracy using the new semiempirical PES. This covers approximately 83% of the energy interval between the rovibrational ground state and the dissociation threshold of water ( $41\,145.94 \text{ cm}^{-1}$ ) (Ref. 23) in the electronic ground state. When combined with information on intensity and line broadening, the new data should allow an accurate modeling of the absorption by atmospheric water monomers essentially through the entire spectrum of solar irradiance.

The authors thank the EPFL, the FNS (Grant Nos. 200020-101475/1 and 200020-112071/1), and the IAP RAS for their generous support of this work, and O. Naymenko for her assistance in assignment of some spectra.

<sup>1</sup>L. Wallace, P. Bernath, W. Livingston, K. Hinkle, J. Busler, B. J. Guo, and K. Q. Zhang, *Science* **268**, 1155 (1995).

<sup>2</sup>F. Allard, P. H. Hauschildt, and D. Schwenke, *Astrophys. J.* **540**, 1005 (2000).

<sup>3</sup>*Climate Change 2001: The Scientific Basis*, edited by J. T. Houghton, Y. Ding, D. J. Griggs, M. Noguer, P. J. Van der Linden, X. Dai, K. Maskell, and C. A. Johnson (Cambridge University Press, Cambridge, 2001).

<sup>4</sup>C. A. Gueymard, *Sol. Energy* **76**, 423 (2004).

<sup>5</sup>C. Camy-Peyret, J. M. Flaud, J. Y. Mandin, J. P. Chevillard, J. Brault, D. A. Ramsay, M. Vervloet, and J. Chauville, *J. Mol. Spectrosc.* **113**, 208 (1985).

<sup>6</sup>J. Y. Mandin, J. P. Chevillard, C. Camy-Peyret, J. M. Flaud, and J. W. Brault, *J. Mol. Spectrosc.* **116**, 167 (1986).

<sup>7</sup>P. F. Coheur, S. Fally, M. Carleer, C. Clerbaux, R. Colin, A. Jenouvrier,

- M. F. Merienne, C. Hermans, and A. C. Vandaele, *J. Quant. Spectrosc. Radiat. Transf.* **74**, 493 (2002).
- <sup>8</sup>M. Tanaka, M. Snee, W. Ubachs, and J. Tennyson, *J. Mol. Spectrosc.* **226**, 1 (2004).
- <sup>9</sup>P. F. Coheur, P. F. Bernath, M. Carleer, R. Colin, O. L. Polyansky, N. F. Zobov, S. V. Shirin, R. J. Barber, and J. Tennyson, *J. Chem. Phys.* **122**, 074307 (2005).
- <sup>10</sup>P. Dupre, T. Gherman, N. F. Zobov, R. N. Tolchenov, and J. Tennyson, *J. Chem. Phys.* **123**, 154307 (2005).
- <sup>11</sup>H. Partridge and D. W. Schwenke, *J. Chem. Phys.* **106**, 4618 (1997).
- <sup>12</sup>G. Li and H. Guo, *J. Mol. Spectrosc.* **210**, 90 (2001).
- <sup>13</sup>O. L. Polyansky, A. G. Csaszar, S. V. Shirin, N. F. Zobov, P. Barletta, J. Tennyson, D. W. Schwenke, and P. J. Knowles, *Science* **299**, 539 (2003).
- <sup>14</sup>S. V. Shirin, O. L. Polyansky, N. F. Zobov, R. I. Ovsyannikov, A. G. Csaszar, and J. Tennyson, *J. Mol. Spectrosc.* **236**, 216 (2006).
- <sup>15</sup>O. V. Boyarkin and T. R. Rizzo, *J. Chem. Phys.* **103**, 1985 (1995).
- <sup>16</sup>R. J. Barnes, A. F. Gross, and A. Sinha, *J. Chem. Phys.* **106**, 1284 (1997).
- <sup>17</sup>J. Tennyson, N. F. Zobov, R. Williamson, O. L. Polyansky, and P. F. Bernath, *J. Phys. Chem. Ref. Data* **30**, 735 (2001).
- <sup>18</sup>D. Hausler, P. Andresen, and R. Schinke, *J. Chem. Phys.* **87**, 3949 (1987).
- <sup>19</sup>R. L. Vanderwal and F. F. Crim, *J. Phys. Chem.* **93**, 5331 (1989).
- <sup>20</sup>J. Tennyson, M. A. Kostin, P. Barletta, G. J. Harris, O. L. Polyansky, J. Ramanlal, and N. F. Zobov, *Comput. Phys. Commun.* **163**, 85 (2004).
- <sup>21</sup>P. Barletta, S. V. Shirin, N. F. Zobov, O. L. Polyansky, J. Tennyson, and A. G. Csaszar, *J. Chem. Phys.* **125**, 204307 (2006).
- <sup>22</sup>S. V. Shirin, O. L. Polyansky, N. F. Zobov, P. Barletta, and J. Tennyson, *J. Chem. Phys.* **118**, 2124 (2003).
- <sup>23</sup>P. Maksyutenko, T. R. Rizzo, and O. V. Boyarkin, *J. Chem. Phys.* **125**, 181101 (2006).